



Evaluation of six precipitation products in the Mekong River Basin

Wei Tian^{a,b}, Xiaomang Liu^{a,*}, Kaiwen Wang^{a,b}, Peng Bai^a, Kang Liang^a, Changming Liu^a

^a Key Laboratory of Water Cycle & Related Land Surface Process, Institute of Geographic Sciences and Natural Resources Research, Chinese Academy of Sciences, 100101 Beijing, China

^b University of Chinese Academy of Sciences, Beijing, China

ARTICLE INFO

Keywords:

Precipitation evaluation
Reference gauge method
Hydrological model
The Mekong River Basin

ABSTRACT

Continuous and reliable precipitation records are essential for hydrological and meteorological studies. In the Mekong River Basin (MRB), there are many satellite-based and gauge-based precipitation products. It is necessary to evaluate the reliabilities of these precipitation products. In this study, we evaluated six widely used precipitation products in the MRB on a monthly scale, namely Asian Precipitation Highly Resolved Observational Data Integration Towards Evaluation of water resources v1101 (APHRODITE), Global Precipitation Climatology Center v2018 (GPCC), Climatic Research Unit Time-Series v4.03 (CRU), Climate Hazards group InfraRed Precipitation with Stations v2.0 (CHIRPS), Multi-Source Weighted-Ensemble Precipitation v1.0 (MSWEP), and Precipitation Estimation from Remotely Sensed Information using Artificial Neural Networks-Climate Data Record (PERSIANN-CDR). Two evaluation methods, namely the reference gauge method and the hydrological simulation method, were used. For the reference gauge method, APHRODITE had the best consistency with precipitation observations at 25 reference gauges among the six precipitation products. For the hydrological simulation method, hydrological model using APHRODITE as the input obtained the most accurate runoff simulations among the six precipitation products. Thus, APHRODITE could be a reliable precipitation product in the MRB. The evaluation results provide a useful reference for the hydrological and meteorological study in the MRB.

1. Introduction

Precipitation is a crucial component of the hydrological cycle, accurate and reliable precipitation records are essential for hydrological simulations, water resources management, and forecasting of extreme hydrological events (Tapiador et al., 2012; Bai et al., 2020). To date, there are three typical methods for precipitation measurements, namely the rain gauge, the weather radar, and the satellite remote sensing. The rain gauge can directly observe precipitation on the ground, and the observations are accurate and reliable at the site scale (Xie and Arkin, 1996; Zhang et al., 2019a). The weather radar can provide real-time precipitation observations with a high temporal and spatial resolution at the regional scale (Ciach et al., 2007; Mei et al., 2014). The satellite remote sensing can measure precipitation using the visible/infrared (VIS/IR)-based methods, the active and passive microwave (MW) techniques, and merged VIS/IR and MW approaches at the quasi-global and global scale (Michaelides et al., 2009; Prigent, 2010; Shao et al., 2019). Based on the three methods, precipitation products with different spatial and temporal resolutions have been developed. Among these

precipitation products, gauge-based and satellite-based precipitation products are widely used. Long-term gauge-based precipitation products mainly include the Climate Research Unit (CRU, Harris et al., 2014; New et al., 2000), the Global Precipitation Climatology Centre (GPCC, Rudolf et al., 2010; Schamm et al., 2014), and others. These products are based on a large number of gauge observation networks (Houghton et al., 2012; Kidd et al., 2017), such as the national meteorological agencies (NMAs), the Global Telecommunication System (GTS), and the Global Climate Observing System, the Food and Agriculture Organization (FAO). Long-term satellite-based precipitation products mainly include the Climate Hazards group Infrared Precipitation with Stations (CHIRPS, Funk et al., 2015), the Multi-Source Weighted-Ensemble Precipitation (MSWEP, Beck et al., 2017, 2019), and the Precipitation Estimation from Remotely Sensed Information using Artificial Neural Networks-Climate Data Record (PERSIANN-CDR, Hsu et al., 1997). Satellite-based precipitation products typically use observations at rain gauges to improve accuracy (Li et al., 2015). Though many precipitation products have been developed, precipitation estimations from different products are often inconsistent owing to different data sources, quality control

* Corresponding author.

E-mail address: liaoxfm@163.com (X. Liu).

<https://doi.org/10.1016/j.atmosres.2021.105539>

Received 18 August 2020; Received in revised form 19 February 2021; Accepted 19 February 2021

Available online 24 February 2021

0169-8095/© 2021 Elsevier B.V. All rights reserved.

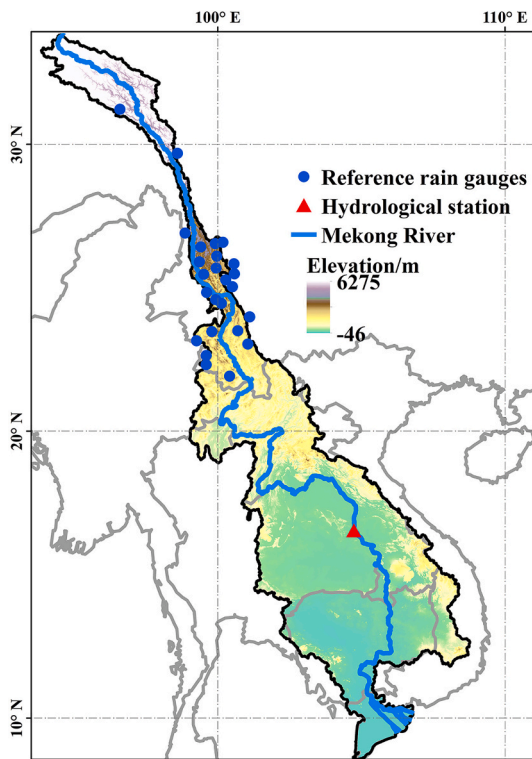


Fig. 1. The location of the Mekong River Basin. The blue dots denote reference rain gauges, and the red triangle denotes the Mukdahan hydrological station.

schemes, and estimation procedures. Consequently, it is necessary to evaluate the reliabilities of different precipitation products.

The reliabilities of precipitation products are generally evaluated by two methods, namely the reference gauge method and the hydrological simulation method. For the reference gauge method, precipitation products are directly compared with observations at the reference gauges (e.g., Hirpa et al., 2010; Buarque et al., 2011; Bumke et al., 2016; Zhang and He, 2016; Akinsanola et al., 2017; Bai and Liu, 2018). These reference gauges should be independent, and not be used during the development of these precipitation products. For the hydrological simulation method, it takes precipitation products as inputs of hydrological models and evaluates the reliabilities of precipitation products through the accuracies of runoff simulations (Salathé Jr, 2003; Behrangi et al., 2011; Bitew and Gebremichael, 2011; Falck et al., 2015; Zhang et al., 2019b). The method is based on the assumption that errors in precipitation products could be propagated into runoff simulations through hydrological models.

The Mekong River is an essential transboundary river in South Asia, and it flows through six countries, namely China, Myanmar, Laos, Thailand, Cambodia, and Vietnam. More than 60 million people in the six countries live in the Mekong River Basin (MRB), and relevant sources of livelihood for these people are agriculture and fisheries (Pech and Sunada, 2008; Piesse, 2016). Agriculture and fisheries are highly

dependent on rainfall, and precipitation is vital for the livelihood of people inhabiting in the MRB. Due to the differences in data sharing strategies across the six countries, long-term precipitation records at the rain gauges are not easily obtained in the MRB. Thus, different precipitation products were widely used in the MRB (Kingston et al., 2011; Chen et al., 2018). Precipitation estimations from different products are inconsistent, and it is necessary to evaluate the reliabilities of different precipitation products in the MRB.

In this study, six satellite-based and gauge-based precipitation products were evaluated by two evaluation methods, namely the reference gauge method and the hydrological simulation method. The rest of the paper is organized as follows. Section 2 introduces the study area and data used, and Section 3 introduces the evaluation methods. Section 4 shows the evaluation results of the six precipitation products by the two evaluation methods. Sections 5 and 6 are the discussion and the conclusions, respectively.

2. Study area and data

2.1. Study area

The Mekong River is one of the most prominent rivers in the world, with a length of 4909 km and an area of 795,000 km² (MRC, 2010). The Mekong River originates from the Tibetan Plateau in China, then flows into Myanmar, Laos, Thailand, Cambodia, Vietnam, and finally ends in the South China Sea Fig. 1. Generally, the Mekong River Basin is divided into two parts, namely the Upper Mekong Basin (UMB) located in China, and the Lower Mekong Basin (LMB) from the Chinese border to the South China Sea. The UMB and LMB account for 24% and 76% of the total area of MRB, respectively (MRC, 2010).

The mean annual runoff of the MRB is approximately 600 mm, and the mean annual precipitation is around 1370 mm (MRC, 2010). The climate is primarily dominated by the tropical monsoon, resulting in a wet season and a dry season within a hydrologic year. The wet season is from May to October and mainly affected by the Indian Summer Monsoon (ISM). The precipitation of the wet season accounts for about 70% of the annual precipitation. The dry season is from November to April of the following year and mainly affected by the East Asian Monsoon (EAM). The precipitation of the dry season accounts for about 30% of the annual precipitation. Besides the ISM and EAM, the MRB is also affected by the Tropical Cyclones (MRC, 2010).

2.2. Precipitation products

In this study, six precipitation products were employed, including three gauge-based precipitation products and three satellite-based precipitation products. The three gauge-based precipitation products are the version of Asian Precipitation Highly Resolved Observational Data Integration Towards Evaluation of water resources v1101 (APHRODITE, Yatagai et al., 2012), the version of Global Precipitation Climatology Center v2018 (GPCC, Schneider et al., 2018), and the version of Climatic Research Unit Time-Series v4.03 (CRU, Harris et al., 2014). The three satellite-based precipitation products are the version of Climate Hazards group InfraRed Precipitation with Stations v2.0 (CHIRPS, Funk et al.,

Table 1

The information about the six precipitation products.

	Name	Time range	Time resolution	Spatial resolution	Data sources
Gauge-based products	APHRODITE	1951–2015	Daily	0.25° × 0.25°	http://www.chikyu.ac.jp/precip/english/index.html
	GPCC	1891–2016	Monthly	0.25° × 0.25°	https://www.dwd.de/EN/ourservices/gpcc/gpcc.html
	CRU	1901–2018	Monthly	0.5° × 0.5°	http://www.cru.uea.ac.uk/data
Satellite-based products	CHIRPS	1981–2017	Daily	0.25° × 0.25°	https://www.chc.ucsb.edu/data/chirps
	PERSIANN-CDR	1983–2017	Daily	0.25° × 0.25°	https://catalog.data.gov/dataset/noaa-climate-data-record-cdr-of-precipitation-estimation-from-remotely-sensed-information-using
	MSWEP	1979–2014	Daily	0.25° × 0.25°	https://platform.princetonclimate.com/PCA_Platform/mswepRetroRequest.html

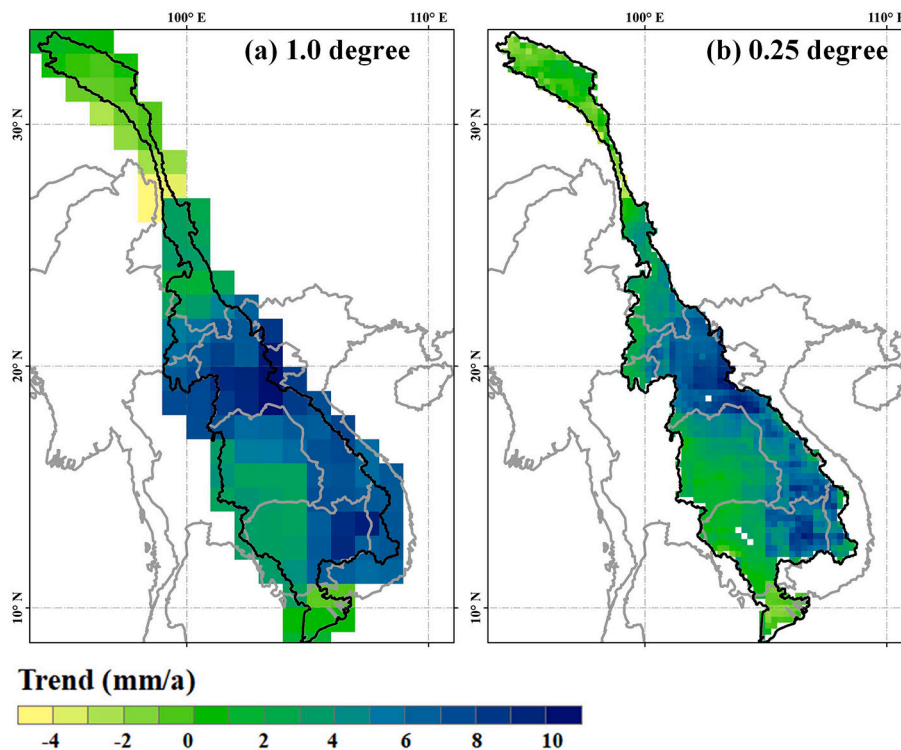


Fig. 2. The trends of terrestrial water storage change in the MRB based on the original (a) and downscaled (b) GRACE data from 2002 to 2016.

2015), the version of Multi-Source Weighted-Ensemble Precipitation v1.0 (MSWEP, Beck et al., 2017), and the Precipitation Estimation from Remotely Sensed Information using Artificial Neural Networks-Climate Data Record (PERSIANN-CDR, Ashouri et al., 2015). Table 1 summarizes the information of the six precipitation products. Note that the spatial and temporal resolutions of the six products are different (Table 1). For spatial resolutions, CRU is $0.5^\circ \times 0.5^\circ$, while the other five products are $0.25^\circ \times 0.25^\circ$. To make them comparable, CRU was resampled at the spatial resolution of $0.25^\circ \times 0.25^\circ$. For temporal resolutions, GPCP and CRU are monthly scales, and the other four products are daily scales. To make them comparable, the four daily precipitation products, namely APHRODITE, CHIRPS, PERSIANN-CDR and MSWEP, were accumulated to the monthly scale.

APHRODITE, produced by the Research Institute for Humanity and Nature and the Meteorological Research Institute of Japan Meteorological Agency, is a long-term and continental-scale daily precipitation product covering Asia (Yatagai et al., 2012). The product is developed based on daily precipitation records from numerous meteorological stations across Asia. These precipitation records are mainly obtained from the GTS, individual collections, and existing meteorological station record datasets, such as the Global Historical Climatology Network (GHCN), and the National Climatic Data Center (NCDC), etc. The version of APHRODITE v1101 was used in this study.

GPCP dataset, produced by the Global Precipitation Climatology Center, is a long-term and global-scale monthly precipitation dataset (Schneider et al., 2018). The dataset is developed based on monthly precipitation records from numerous meteorological stations across the world. These records are primarily obtained from the NMAs, the GTS, the Climatic Research Unit, the FAO, the GHCN, and others. The version of the GPCP v2018 was used in this study.

CRU dataset, produced by the University of East Anglia, is a long-term and global-scale monthly climate variables product (Harris et al., 2014). The product is developed based on monthly meteorological records from numerous meteorological stations across the world. These records are mainly obtained from the NMAs, the World Meteorological Organization, the Climatic Research Unit, the Centro Internacional de

Agricultura Tropical, the FAO, and others. The version of the CRU TS v4.03 was used in this study.

CHIRPS, produced by the U.S. Geological Survey and the Climate Hazards Group at the University of California, Santa Barbara, is a long-term and quasi-global (50°S - 50°N) daily precipitation product (Funk et al., 2015). This product combines the pentad precipitation climatology, quasi-global geostationary thermal infrared satellite observations from the Climate Prediction Center (CPC) and the NCDC, atmospheric model rainfall fields from the NOAA Climate Forecast System version 2, and precipitation observations from the GTS and the GHCN. The version of the CHIRPS v2.0 was used in this study.

PERSIANN-CDR, produced by the University of California in Irvine, is a long-term and quasi-global (60°S - 60°N) daily precipitation product (Ashouri et al., 2015). This product estimates precipitation by calculating GridSat-B1 IR satellite data using an artificial neural network model, the PERSIANN algorithm. The artificial neural network is trained with stage IV hourly precipitation data from the NCEP. Besides, the PERSIANN-CDR also uses precipitation data from the Global Precipitation Climatology Project to improve the accuracy of precipitation estimation.

MSWEP, produced by the group of Beck (Beck et al., 2017), is a long-term and global-scale daily precipitation product. This product takes advantage of the strengths of gauge, satellite, and reanalysis-based data. The data sources mainly include seven datasets, namely CPC, GPCP, CMORPH, GSMaP-MVK, 3B42RT, ERA-Interim, and JRA-55. In addition, the correction for gauge under-catch and orographic effects is introduced by inferring catchment-average precipitation from runoff observations at 13,762 stations across the world. The version of the MSWEP v1.0 was used in this study.

2.3. Other data

The reliabilities of precipitation products are evaluated by the reference gauge method and the hydrological simulation method. For the reference gauge method, the monthly precipitation observations at 25 reference gauges in China from 1984 to 2014 are obtained from the

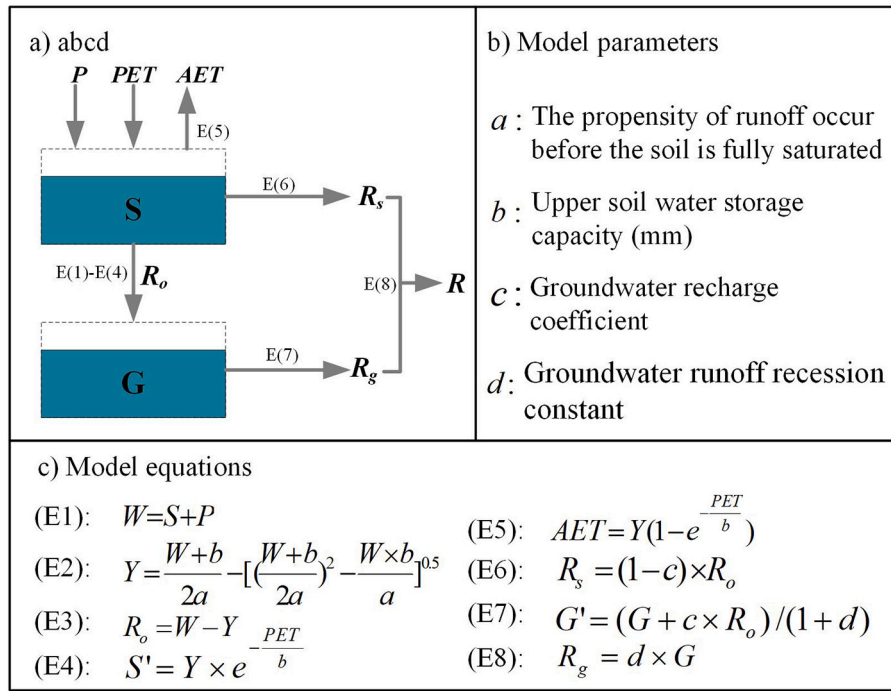


Fig. 3. Structures and key equations of the abcd model.

China Meteorological Administration (<http://data.cma.cn/>, Fig. 1). These precipitation observations have been subject to strict quality control. We note that the precipitation observations at the 25 stations were not used during the development of the six precipitation products. For the hydrological simulation method, the monthly runoff observations of Mukdahan hydrological station from 1984 to 2008 were obtained from the Mekong River Commission (<https://portal.mrcmekong.org/home>). We note that constructions of the reservoirs have significantly affected runoff observations in the MRB since 2009. Thus, 2008 was selected as the last year of the hydrological simulation in this study. Monthly potential evapotranspiration data during 1984 to 2008 were from the Global Land Data Assimilation System v3.3a (<https://www.gleam.eu/#datasets>). The Release 6.0 monthly Gravity Recovery and Climate Experiment (GRACE) product provided by the University of Texas Center for Space Research were used (<http://grace.jpl.nasa.gov>). The time range of the product is from April 2002 to January 2017, and the spatial resolution is $1^\circ \times 1^\circ$. Because the GRACE data have a coarse spatial resolution, a statistical downscaling approach based on a land surface model (LSM) was used to downscale the GRACE data (Wan et al., 2015; Zhang et al., 2019). The approach combines the advantages of GRACE and LSM in the estimations of total water storage change (TWSC). LSM can provide better spatial patterns of TWSC than GRACE data, while values of LSM-simulated TWSC have uncertainties. Here, the $0.25^\circ \times 0.25^\circ$ dataset of TWSC simulated by the Noah model in the MRB (<https://disc.gsfc.nasa.gov/datasets?keywords=GLDAS>) was employed as weighting factors in each $1.0^\circ \times 1.0^\circ$ grid element to downscale TWSC data from GRACE. This downscaling approach ensures that the sum of the downscaled TWSC in each $1.0^\circ \times 1.0^\circ$ grid is equal to the corresponding $1.0^\circ \times 1.0^\circ$ grid GRACE-estimated TWSC. The original and downscaled trends of the GRACE-estimated TWSC from 2002 to 2016 are shown in Fig. 2. The downscaled TWSC shows a similar spatial pattern with the original GRACE-estimated TWSC, but with a finer resolution. Wan et al. (2015) described the approach of downscaling GRACE data in detail.

3. Methodology

3.1. Evaluation methods and indices

The reliabilities of six precipitation products were evaluated by two methods, namely the reference gauge method and the hydrological simulation method (Bai et al., 2018). For the reference gauge method, the precipitation observations of the reference gauges were compared with the precipitation estimations of corresponding grids for the precipitation products, and the values of evaluation indices were calculated in each gauge (Frei et al., 2003). For the hydrological simulation method, the hydrological model used the precipitation products as inputs to simulate runoff, and the reliabilities of precipitation products were evaluated by the accuracies of runoff simulations (Behrangi et al., 2011). Here, the hydrological model used is the abcd model. The model was calibrated by two calibration cases, and details are in Section 3.3.

Four evaluation indices were used, namely the Pearson correlation coefficient (CC), percent bias (PBIAS), root-mean-square error (RMSE), and Kling-Gupta efficiency (KGE) (Gupta et al., 2009). The four evaluation indices are calculated as follows:

$$CC = \frac{\sum_{i=1}^N (P_{obs,i} - \bar{P}_{obs}) (P_{sim,i} - \bar{P}_{sim})}{\sqrt{\sum_{i=1}^N (P_{obs,i} - \bar{P}_{obs})^2 \sum_{i=1}^N (P_{sim,i} - \bar{P}_{sim})^2}} \quad (1)$$

$$PBIAS = \frac{\sum_{i=1}^N (P_{obs,i} - P_{sim,i})}{\sum_{i=1}^N P_{obs,i}} \times 100\% \quad (2)$$

$$RMSE = \sqrt{\frac{\sum_{i=1}^N (P_{obs,i} - P_{sim,i})^2}{N}} \quad (3)$$

$$KGE = 1 - \sqrt{(1-r)^2 + (1-\alpha)^2 + (1-\beta)^2} \text{ where } \alpha = \frac{\sigma_s}{\sigma_o}, \beta = \frac{\mu_s}{\mu_o} \quad (4)$$

where $P_{obs,i}$ and $P_{sim,i}$ are observations and simulations on i -th month, respectively. N is the total number of months in the evaluation period. μ_p

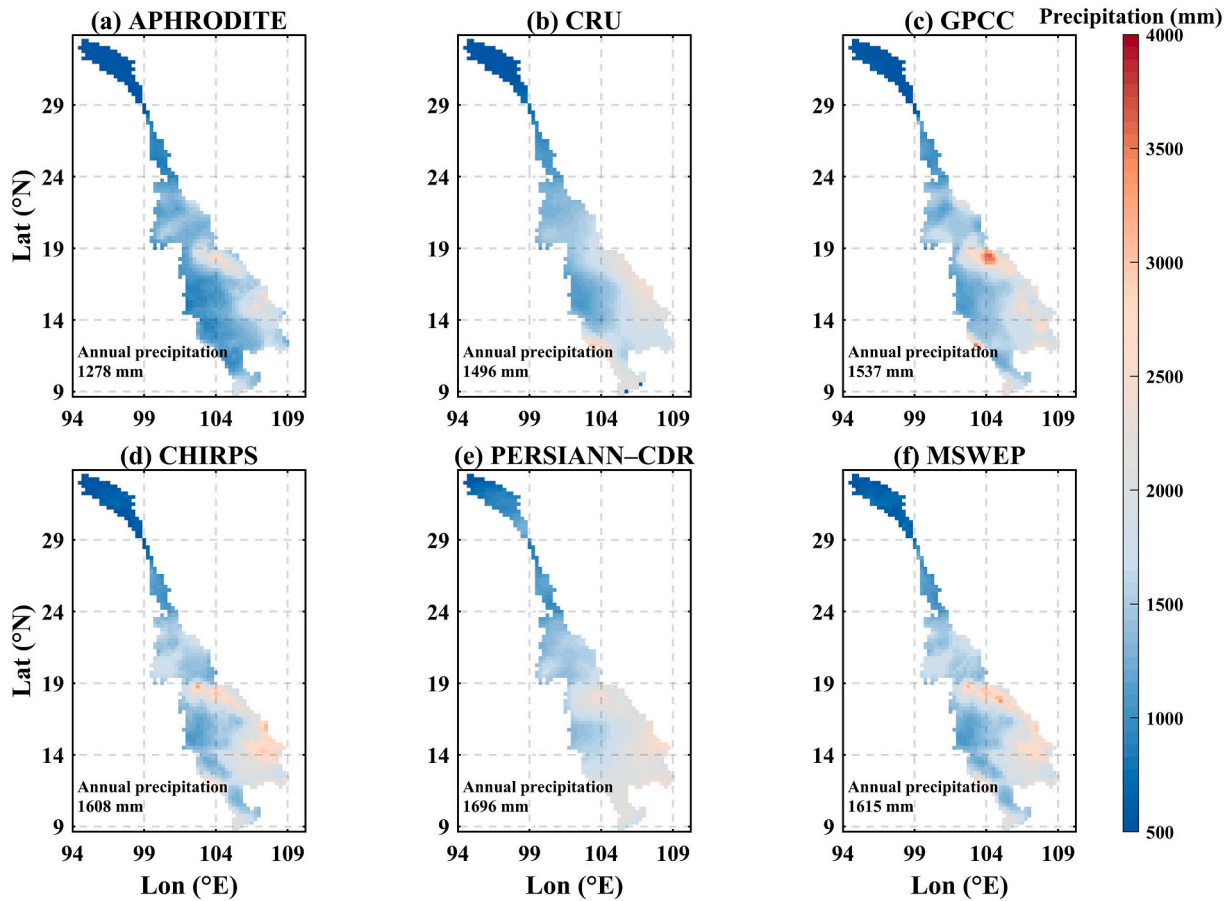


Fig. 4. Spatial patterns of the mean annual precipitation for the six products from 1984 to 2014 in the MRB.

and σ_p are the mean and standard deviation of the simulations, respectively. μ_o and σ_o are the mean and standard deviation of the observations, respectively. r is the correlation coefficient between observations and simulations. The optimal values of the four evaluation indices, namely CC , $PBIAS$, $RMSE$, and KGE , are 1, 0%, 0, and 1, respectively. The negative value of $PBIAS$ indicates the observations being overestimated by the simulations, and vice versa (Moriasi et al., 2007).

3.2. Hydrological model

A monthly conceptual hydrological model, the abcd model, was used to simulate runoff. The abcd model has been used in many basins worldwide with various climatic conditions (Alley, 1984; Gupta et al., 2009; Zhao et al., 2016; Bai et al., 2018; Tian et al., 2018). The structures and equations of the abcd model are listed in Fig. 3. The abcd model has four parameters (a , b , c , d) and divides the storage layer into two layers, namely soil moisture storage and groundwater storage. The model defines two key state variables, namely Y_t as evapotranspiration opportunity and W_t as available water (Thomas, 1981). W_t is the sum of precipitation during month t and soil water storage at the beginning of month t , and Y_t is the sum of actual evapotranspiration (AET) during month t and soil water storage at the end of month t . Y_t is postulated as a nonlinear function of W_t (E2 in Fig. 3). AET is calculated using a nonlinear formula related to Y_t (E5 in Fig. 3). R_s and R_g are calculated using linear formulas related to water available for runoff and groundwater storage, respectively (E6 and E8 in Fig. 3, respectively). Detailed descriptions of the abcd model can be found in Fernandez et al. (2000) and Martinez and Gupta (2010).

3.3. Model calibration and validation

The classic split sample test scheme (Klemes, 1986) was used for calibration and validation of the hydrological model. The available data in the basin was spilled into two sub-periods, namely sub-period I and sub-period II, which were used to calibrate and validate the hydrological model, respectively. Here, two calibration cases were used to calibrate the hydrological model. The first calibration case only used runoff observations to calibrate the hydrological model. The second calibration case used both runoff and $TWSC$ observations to calibrate the hydrological model.

For the first calibration case, the hydrological model was calibrated in sub-period I (1984–1995) and validated in sub-period II (1996–2008). The maximize Nash-Sutcliffe efficiency (NSE , Nash and Sutcliffe, 1970) between simulated and observed runoff was taken as the objective function to calibrate the hydrological model. The NSE is calculated as follows:

$$NSE = 1 - \frac{\sum_{i=1}^n (Q_{obs,i} - Q_{sim,i})^2}{\sum_{i=1}^n (Q_{obs,i} - \bar{Q}_{obs})^2} \quad (5)$$

where Q_{obs} and Q_{sim} are the observed and simulated monthly runoff, respectively; \bar{Q}_{obs} is the mean of the observed monthly runoff, n is the total number of time steps. The global optimization algorithm, namely the genetic algorithm (Boyle et al., 2000), was used to find the parameter sets of the abcd model. This algorithm is a robust and efficient search algorithm that has been widely used to calibrate hydrological models (Tolson and Shoemaker, 2007).

For the second calibration case, the hydrological model was

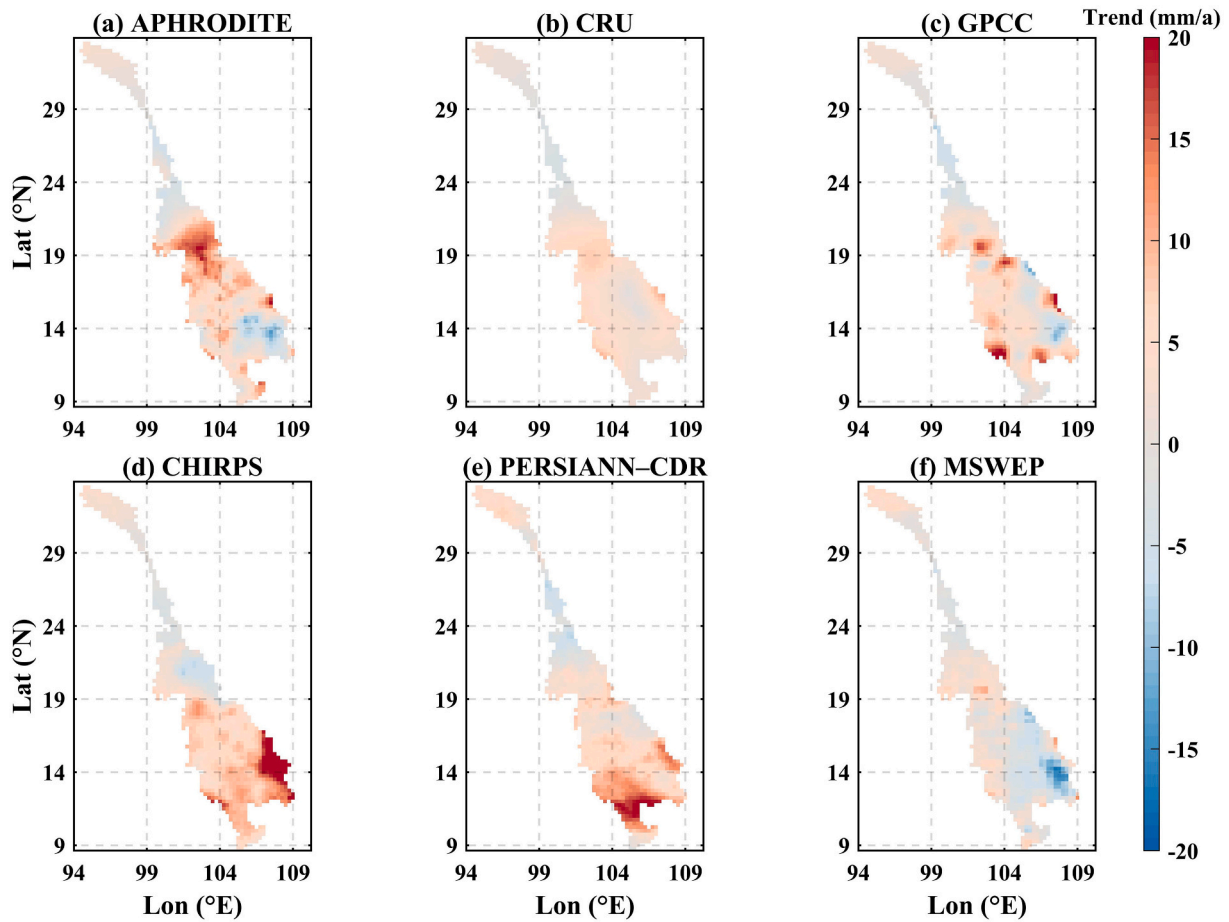


Fig. 5. Spatial patterns of the annual precipitation trend from 1984 to 2014 for the six products in the MRB.

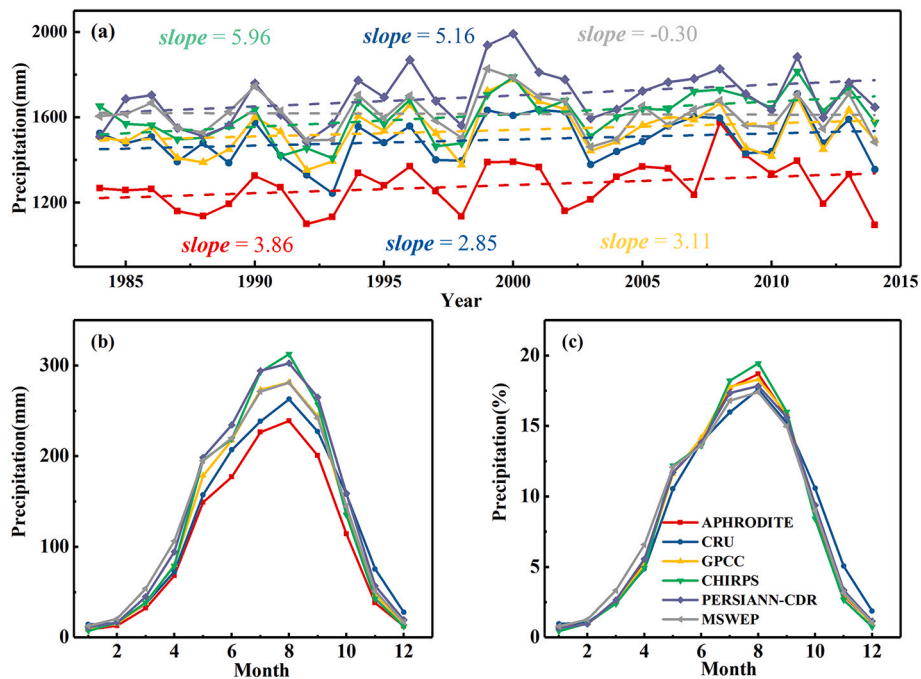


Fig. 6. The temporal variability of the six precipitation products in the MRB: (a) time series of annual precipitation for each product from 1984 to 2014; (b) mean monthly precipitation for each product; (c) contribution rate of mean monthly precipitation to mean annual precipitation for each product.

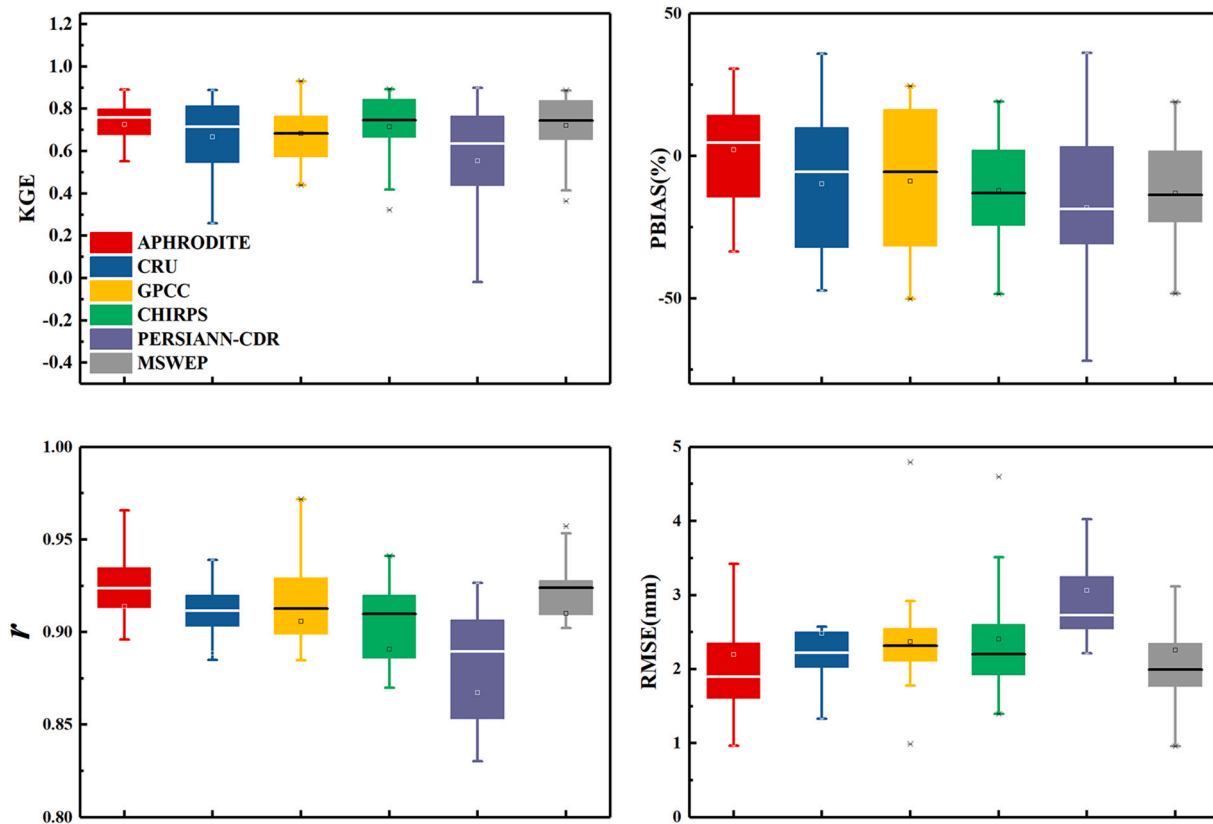


Fig. 7. Evaluation results of the reference gauge method for the six precipitation products at 25 reference stations from 1984 to 2014. In the boxplots, the outer edges of the boxes and the horizontal lines within the boxes represent the 25th, 75th, and 50th percentiles of the performance statistics, and the lengths of upper and lower whiskers do not exceed 1.5 times the box lengths. (a) *KGE*, Kling-Gupta efficiency; (b) *PBIAS*, Percent bias; (c) *CC*, Pearson correlation coefficient; (d) *RMSE*, Root-mean-square error.

calibrated by runoff and *TWSC* observations. *TWSC* observations estimated by *GRACE* began in 2002. Thus, the hydrological model was calibrated in sub-period I (2002–2005) and validated in sub-period II (2006–2008). The maximize *NSE* between simulated and observed runoff and maximize *NSE* between simulated and observed *TWSC* were taken as objective functions to calibrate the hydrological model simultaneously. The calibration case is a multi-objective optimization, involving two conflicting objective functions to be optimized simultaneously (Gupta et al., 1999). The non-dominated sorting genetic algorithm II was used to find the parameter sets of the abcd model (Srinivas and Deb, 1994). This algorithm is commonly used in multi-objective optimization (Deb et al., 2002; Werth et al., 2009).

4. Results

4.1. Inter-comparisons of the six precipitation products

Fig. 4 shows spatial patterns of mean annual precipitation of the six products, namely APHRODITE, CRU, GPCC, CHIRPS, PERSIANN-CDR, and MSWEP, in the MRB from 1984 to 2014. Generally, different products have similar spatial distribution of precipitation, showing an increasing trend from northwest to southeast. However, there are significant differences in the values of mean annual precipitation among the six precipitation products. Mean annual precipitations of the six products are 1278 mm, 1492 mm, 1537 mm, 1608 mm, 1696 mm, and 1615 mm, respectively. Fig. 5 shows spatial patterns of annual precipitation trends of the six products in the MRB from 1984 to 2014. The six products have similar spatial distribution in the northwestern and central regions, and different spatial distribution in the southeastern region. The six products all show that annual precipitation has a downward

trend in the northwestern region and an upward trend in the central region. APHRODITE, CRU, GPCC, and MSWEP show that annual precipitation has a downward trend in the southeastern region, while CHIRPS and PERSIANN-CDR show that annual precipitation has an upward trend in the southeastern region.

Fig. 6 shows the temporal variability of the six precipitation products in the MRB from 1984 to 2014. For the time series of annual precipitation, increasing trends of annual precipitation are found in five precipitation products, except MSWEP. The increasing trends of the five precipitation products range from 2.85 mm/a to 5.96 mm/a, and the decreasing trend of the MSWEP is -0.30 mm/a. For all the six precipitation products, the largest mean monthly precipitation occurs in August, and the smallest mean monthly precipitation occurs in January. For the contribution rate of mean monthly precipitation to mean annual precipitation, the six precipitation products are generally consistent with each other.

4.2. Results of the reference gauge method

The six precipitation products were evaluated using the reference gauge method on a monthly scale. Precipitation observations of the 25 reference gauges were compared with precipitation estimations of corresponding grids for the precipitation products, and the values of evaluation indices were calculated in each gauge. First, the precipitation products were evaluated in whole seasons (Fig. 7). The median values of *KGE* between the observed and estimated precipitation for the six precipitation products, namely APHRODITE, CRU, GPCC, CHIRPS, PERSIANN-CDR, and MSWEP, are 0.76, 0.72, 0.68, 0.75, 0.64 and 0.74, respectively. The median values of *PBIAS* are 4.7%, -5.5% , -5.6% , -13.1% , -18.6% and -13.6% , respectively. The median values of *CC*

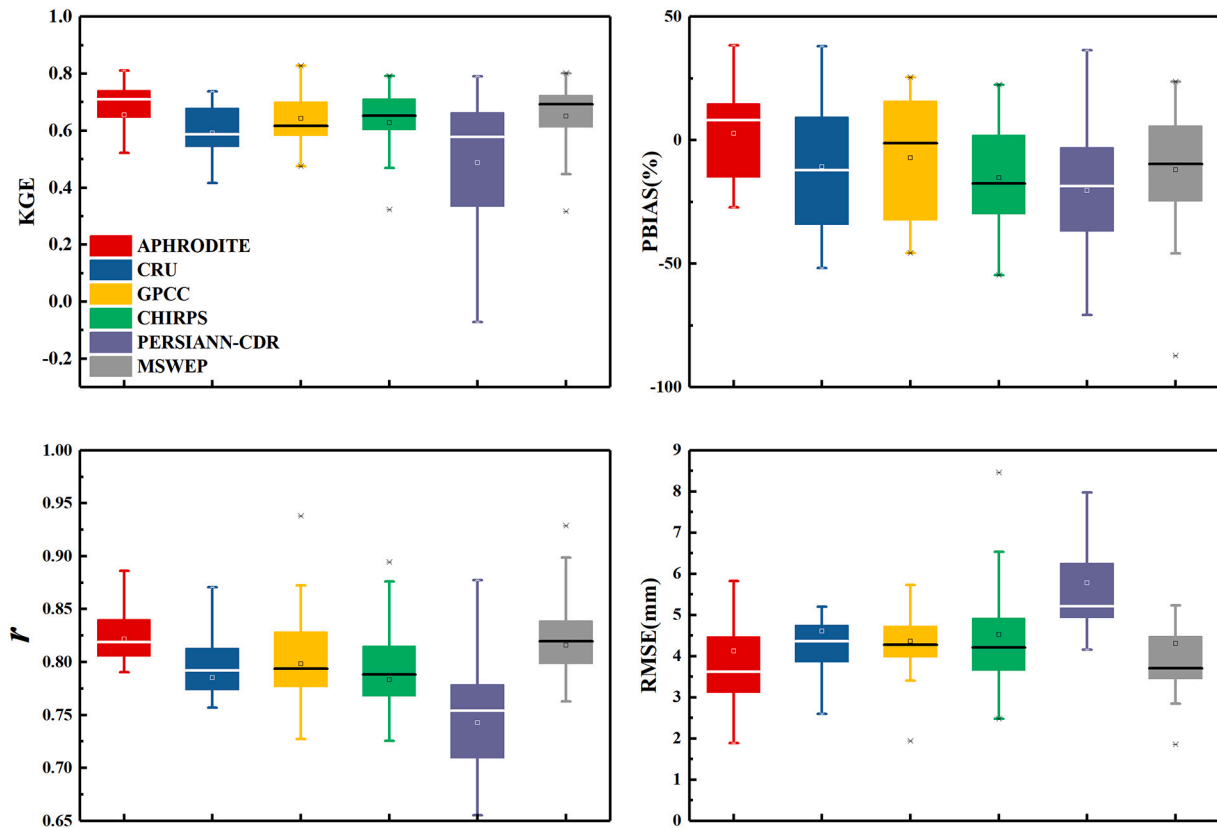


Fig. 8. Evaluation results of the reference gauge method for the six precipitation products at 25 reference stations from 1984 to 2014 during the wet season (from May to October).

are 0.92, 0.91, 0.91, 0.91, 0.88 and 0.92, respectively. The median values of $RMSE$ are 1.89 mm, 2.22 mm, 2.32 mm, 2.20 mm, 2.73 mm, and 1.99 mm, respectively. Generally, APHRODITE has the lowest $PBIAS$ median value, the lowest $RMSE$ median value, and the largest KGE median value among the six precipitation products. Second, the precipitation products were separately evaluated in wet and dry seasons (Figs. 8 and 9, respectively). During the wet season, APHRODITE has the largest KGE median value, the largest CC median value and the lowest $RMSE$ median value among the six precipitation products (Fig. 8). The values of the three evaluation indices were 0.71, 0.82, and 3.62 mm, respectively. GPCP has the lowest $PBIAS$ median value, with a value of -1.2% . During the dry season, APHRODITE has the largest KGE median value, the largest CC median value and the lowest $RMSE$ median value among the six precipitation products (Fig. 9). The values of the three evaluation indices were 0.74, 0.91, and 0.90 mm, respectively. PERSIANN-CDR has the lowest $PBIAS$ median value, with a value of 3.6% . Therefore, APHRODITE has the best consistency with station observations at the 25 reference gauges among the six precipitation products.

4.3. Results of the hydrological simulation method

The first calibration case only used runoff observations to calibrate the abcd hydrological model. Figs. 10 and 11 show the observed and simulated runoff in the Mukdahan station during the calibration period (1984–1995) and the validation period (1996–2008), respectively. First, the runoff simulation was evaluated for the whole seasons (Figs. 10 and 11). The abcd model can well simulate runoff using any of the six precipitation products as inputs during the calibration and validation period. The KGE values between the observed and simulated runoff for the six precipitation products during the calibration period range from 0.82 to 0.89. The corresponding KGE values during the validation period

range from 0.77 to 0.80. The $PBIAS$ values between the observed and simulated runoff for the six precipitation products during the calibration period range from -4.8% to -9.4% . The corresponding $PBIAS$ values during the validation period range from 1.2% to 5.3% . The CC values between the observed and simulated runoff for the six precipitation products during the calibration period range from 0.96 to 0.97. The corresponding CC values during the validation period range from 0.95 to 0.96. The $RMSE$ values between the observed and simulated runoff for the six precipitation products during the calibration period range from 0.94 mm to 1.15 mm. The corresponding $RMSE$ values during the validation period range from 1.34 mm to 1.47 mm. Second, the runoff simulations were separately evaluated in wet and dry seasons (Table 2). During the validation period, the KGE values between the observed and simulated runoff for the six precipitation products during the wet season range from 0.66 to 0.70. The corresponding KGE values during the dry season range from 0.72 to 0.85. The $PBIAS$ values between the observed and simulated runoff for the six precipitation products during the wet season range from 5.4% to 8.5% . The corresponding $PBIAS$ values during the dry season range from -6.7% to -10.6% . The CC values between the observed and simulated runoff for the six precipitation products during the wet season range from 0.91 to 0.94. The corresponding CC values during the dry season range from 0.90 to 0.93. The $RMSE$ values between the observed and simulated runoff for the six precipitation products during the wet season range from 2.61 mm to 2.98 mm. The corresponding $RMSE$ values during the dry season range from 0.50 mm to 0.61 mm.

In conclusion, the values of the four evaluation indices show that there are no significant differences among the accuracies of runoff simulations using the six precipitation products as inputs. A possible explanation is that accurate runoff simulations are obtained at the cost of reducing the simulation accuracies of other hydrological variables, such as AET and $TWSC$. The simulated AET , Q , and $TWSC$ obtained by

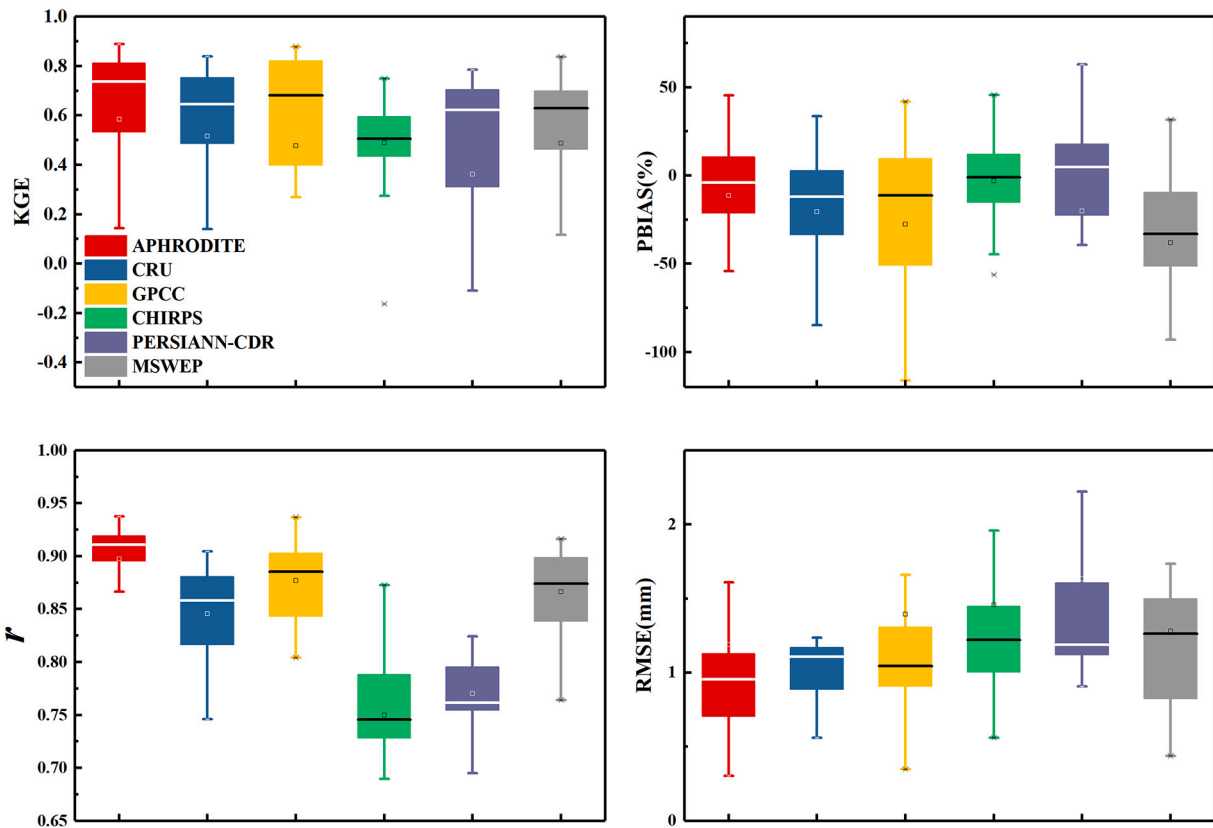


Fig. 9. Evaluation results of the reference gauge method for the six precipitation products at 25 reference stations from 1984 to 2014 during the dry season (from November to April of the following year).

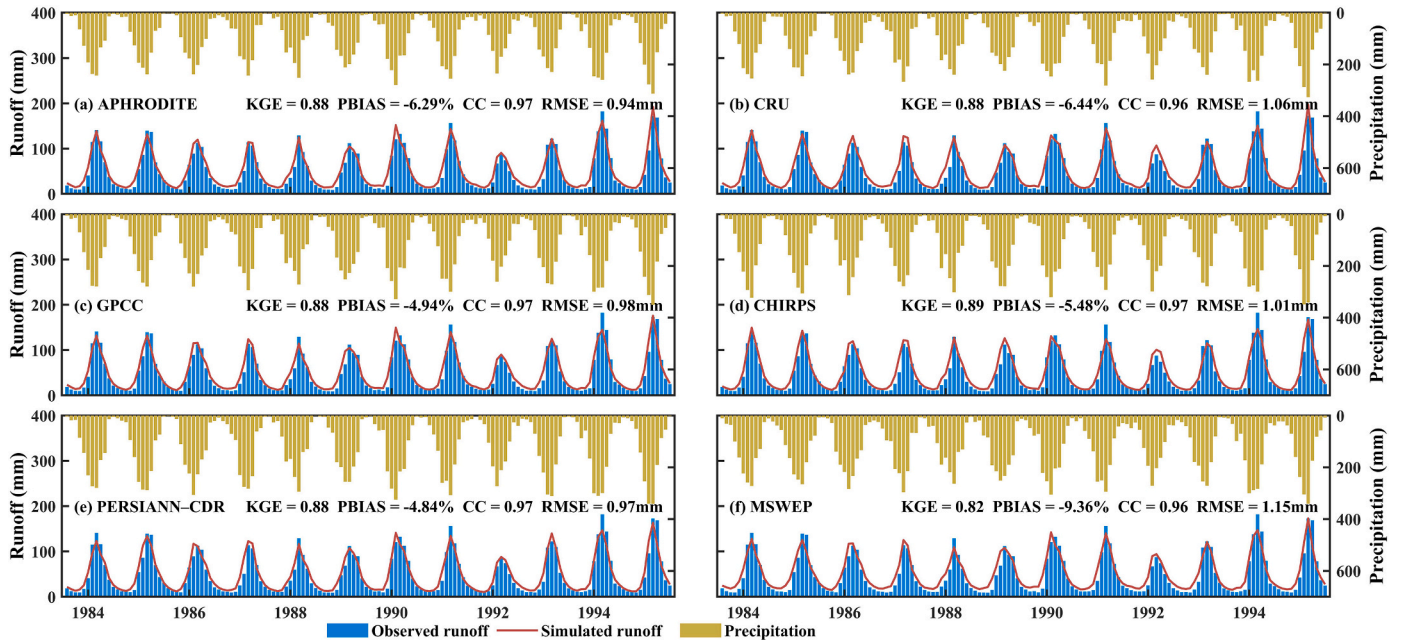


Fig. 10. The monthly observed (Q_{obs}) and simulated (Q_{sim}) runoff hydrographs at the Mukdahan hydrological station during the calibration period (1984–1995) using the six precipitation products as the input. In each panel, precipitation values (right Y axis) are shown from top to bottom.

the abcd model using the six precipitation products as inputs are shown in Fig. 12. With different precipitation products as inputs, the simulated Q are similar to each other, while the simulated AET and $TWSC$ are significantly different. Thus, the reliabilities of precipitation products cannot be evaluated using only runoff observations to calibrate the

hydrological model.

The second calibration case used both runoff and $TWSC$ observations to calibrate the hydrological model. The abcd model was calibrated by both maximizing the NSE between the observed and simulated runoff and the NSE between the observed and simulated $TWSC$. Table 3 shows

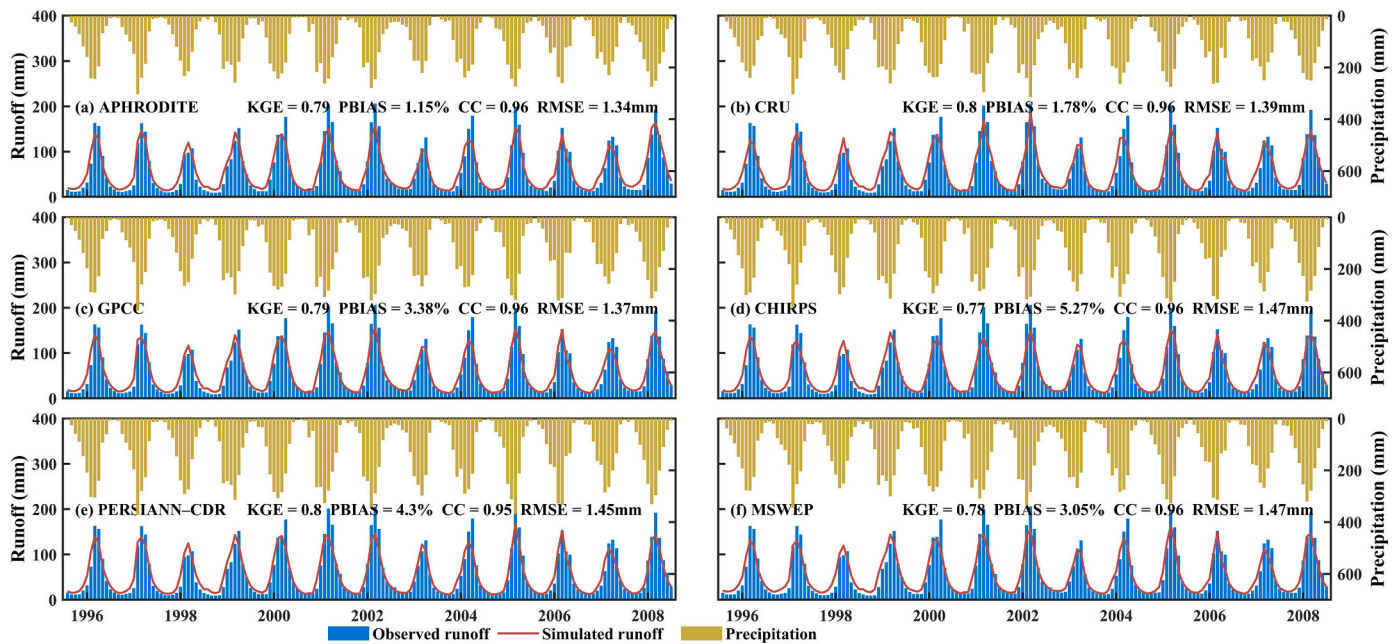


Fig. 11. The monthly observed (Q_{obs}) and simulated (Q_{sim}) runoff hydrographs at the Mukdahan hydrological station during the validation period (1996–2008) using the six precipitation products as the input. In each panel, precipitation values (right Y axis) are shown from top to bottom.

Table 2

The values of the four evaluation indices for the runoff simulations by the abcd model using the six precipitation products as inputs during the wet and dry seasons.

Season		Calibration period (1984–1995)				Validation period (1996–2008)			
		KGE	PBIAS (%)	r	RMSE (mm)	KGE	PBIAS (%)	r	RMSE (mm)
Wet Season	APHRODITE	0.84	-1.9	0.95	1.78	0.70	5.4	0.94	2.61
	CRU	0.80	-2.2	0.92	2.13	0.67	6.0	0.92	2.88
	GPCC	0.80	-1.5	0.94	1.92	0.68	6.3	0.93	2.74
	CHIRPS	0.81	-2.5	0.93	1.98	0.66	8.5	0.92	2.94
	PERSIANN-CDR	0.82	-1.8	0.95	1.82	0.70	6.3	0.92	2.76
	MSWEP	0.73	-2.8	0.92	2.23	0.66	7.3	0.91	2.98
Dry Season	APHRODITE	0.83	-22.9	0.96	0.58	0.82	-10.3	0.91	0.54
	CRU	0.82	-16.9	0.95	0.49	0.85	-9.0	0.92	0.53
	GPCC	0.81	-18.6	0.97	0.48	0.82	-8.4	0.93	0.50
	CHIRPS	0.84	-15.2	0.96	0.44	0.84	-6.7	0.92	0.50
	PERSIANN-CDR	0.76	-23.6	0.97	0.58	0.81	-10.6	0.91	0.56
	MSWEP	0.65	-31.8	0.95	0.77	0.72	-10.6	0.90	0.61

the values of the four evaluation indices between observed and simulated runoff in the Mukdahan station during the calibration period (2002–2005) and the validation period (2006–2008). There are significant differences among the accuracies of runoff simulations using the six precipitation products as inputs. First, the runoff simulation was evaluated for the whole seasons. For the calibration period, the largest value of KGE , the smallest value of $PBIAS$, and the smallest value of $RMSE$ among the six precipitation products are found in APHRODITE, GPCC, and APHRODITE, respectively. There are limited differences (≤ 0.01) among the values of CC among the six precipitation products. For the validation period, the largest value of KGE , the smallest value of $PBIAS$, and the smallest value of $RMSE$ among the six precipitation products are all found in APHRODITE. There are limited differences (≤ 0.02) among the values of CC among the six precipitation products. Second, the runoff simulations were separately evaluated in wet and dry seasons. For the wet season, the largest value of KGE , the smallest value of $PBIAS$, and the smallest value of $RMSE$ among the six precipitation products during the validation period were found in APHRODITE, APHRODITE, and CHIRPS, respectively. There are limited differences (≤ 0.03) among the values of CC among the six precipitation products. For the dry season, the largest value of KGE , the smallest value of $PBIAS$, and the smallest value of $RMSE$ among the six precipitation products

during the validation period were all found in APHRODITE. There are limited differences (≤ 0.03) among the values of CC among the six precipitation products. In short, the hydrological model using APHRODITE as input can obtain the most accurate runoff simulations among the six precipitation products.

5. Discussion

5.1. Comparisons with other studies

In this study, the two evaluation methods both show that APHRODITE has a better performance compared with the other five precipitation products in the MRB. The result is consistent with previous studies. Lutz et al. (2014) and Chen et al. (2017) both found that APHRODITE had relatively high accuracy in the MRB. However, these studies only used the reference gauge method to evaluate different precipitation products. In this study, the six precipitation products were systematically evaluated using the reference gauge method and the hydrological simulation method.

GPCC is typically used to correct satellite-based precipitation products globally. Compared with GPCC, APHRODITE is a precipitation product only covering Asia and was developed using more rain stations

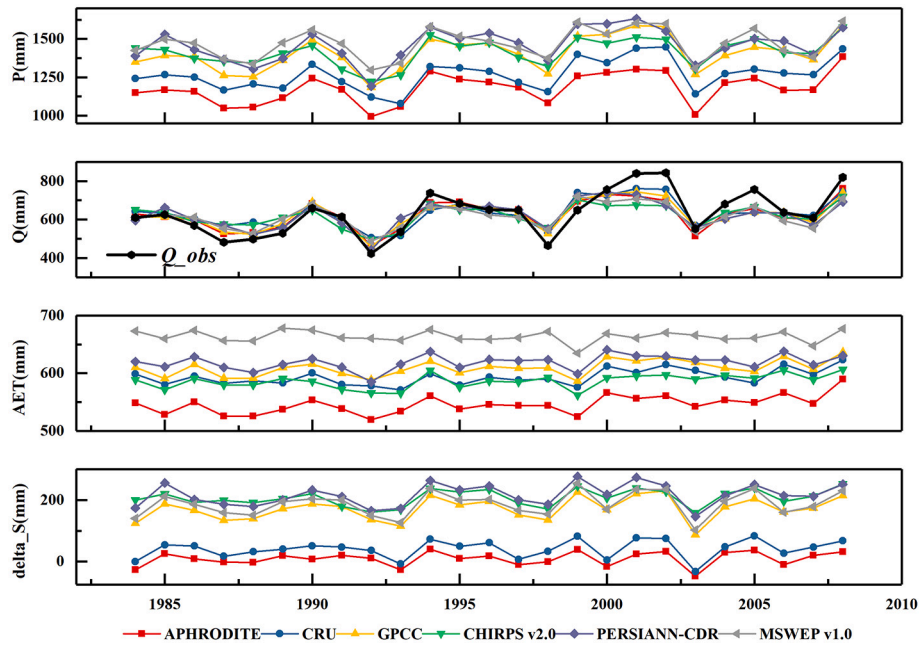


Fig. 12. Simulations of hydrological variables by the abcd model using the six precipitation products as inputs in the MRB.

Table 3

The values of the four evaluation indices for the runoff simulations by the abcd model using the six precipitation products as inputs.

Season		Calibration period (2002–2005)				Validation period (2006–2008)			
		KGE	PBIAS(%)	r	RMSE(mm)	KGE	PBIAS(%)	r	RMSE(mm)
Whole	APHRODITE	0.85	-5.5	0.94	2.96	0.81	3.5	0.94	2.97
	CRU	0.61	8.8	0.95	3.94	0.58	12.7	0.93	4.13
	GPCC	0.75	-1.4	0.95	3.10	0.69	3.5	0.95	3.30
	CHIRPS	0.77	-2.8	0.95	2.97	0.72	3.7	0.94	3.30
	PERSIANN-CDR	0.78	-8.1	0.95	3.08	0.72	3.9	0.95	3.15
	MSWEP	0.72	2.3	0.95	3.31	0.67	3.6	0.94	3.52
Wet Season	APHRODITE	0.61	-1.5	0.93	5.83	0.65	-3.1	0.94	5.74
	CRU	0.41	19.0	0.92	8.17	0.40	15.3	0.97	7.73
	GPCC	0.51	9.0	0.95	6.46	0.54	3.4	0.95	5.98
	CHIRPS	0.53	5.6	0.93	6.43	0.57	3.5	0.94	5.73
	PERSIANN-CDR	0.55	8.0	0.94	6.22	0.57	-7.0	0.94	5.79
	MSWEP	0.48	8.8	0.94	6.92	0.51	6.8	0.94	6.44
Dry Season	APHRODITE	0.69	-12.7	0.95	1.12	0.81	-15.0	0.91	1.48
	CRU	0.57	-17.1	0.96	1.15	0.79	-19.0	0.93	1.48
	GPCC	0.53	-22.2	0.95	1.33	0.76	-21.6	0.93	1.60
	CHIRPS	0.51	-22.5	0.93	1.44	0.76	-21.1	0.93	1.54
	PERSIANN-CDR	0.65	-15.2	0.94	1.05	0.67	-28.9	0.90	2.12
	MSWEP	0.62	-21.9	0.92	1.33	0.78	-16.7	0.90	1.54

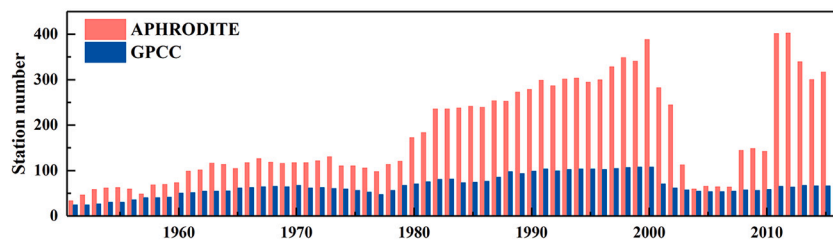


Fig. 13. Maximum numbers of meteorological station used to develop the precipitation product for GPCC and APHRODITE in the MRB from 1951 to 2015.

in Asia from 1951 to 2015. Fig. 13 shows that the maximum numbers of meteorological stations used to develop the precipitation product in the MRB are 388 and 107 for APHRODITE and GPCC, respectively. Thus, APHRODITE could be a more reliable precipitation product in the MRB.

5.2. Uncertainty

There are several uncertainties in the evaluation methods used in this study. First, the reference gauge method has its uncertainties due to the scale mismatch between the precipitation products and meteorological station observations. It is difficult for a single station to represent a grid

($0.25^\circ \times 0.25^\circ$) of precipitation, particularly in mountain regions. Second, the 25 independent reference gauges used in this study are all located in the upper Mekong River Basin (UMRB), because the observations of independent stations in the lower Mekong River Basin (LMRB) cannot be obtained. This may lead to uncertainty in the results of the reference gauge method. To evaluate the performance of precipitation products throughout the MRB, this study also used the hydrological simulation method in addition to the reference gauge method. For the hydrological simulation method, the hydrological station, namely the Mukdahan station, is located in the LMRB. The evaluation results of the two methods are consistent. Thus, using independent gauges located in the UMRB could not affect the conclusion of this study. Third, the hydrological simulation method also has its uncertainties, such as the structure of the hydrological model. The abcd model does not simulate the impact of human activities on hydrological processes (Cai et al., 2015; Clark et al., 2016; Yang et al., 2017). In the MRB, the main impacts of human activities on hydrological processes are reservoir constructions, such as Nuozadu and Xiaowan reservoir. These huge reservoirs were built after 2009, while the runoff simulations were conducted before 2009 in this study. Thus, the impacts of reservoir constructions on hydrological simulations are limited.

6. Conclusions

The objective of the study is to evaluate the six long-term precipitation products in the MRB. To fulfill this objective, the six precipitation products were evaluated by the two methods, namely the reference gauge method and the hydrological simulation method. The main conclusions are summarized as follows.

1. The six precipitation products have similar spatial patterns, while the mean annual precipitation and annual precipitation trends demonstrate significant differences. The mean annual precipitation of the six products range from 1278 mm to 1696 mm, and the annual precipitation trends of the six products range from -0.30 mm/a to 5.96 mm/a.
2. For the reference gauge method, APHRODITE has the best consistency with the observations at the 25 reference gauges, with the lowest median value of *RMSE*, and the largest median value of *KGE* among the six precipitation products.
3. For the hydrological simulation method, the six precipitation products were used as inputs of the abcd hydrological model. Runoff and *TWSC* observations were used together to calibrate the hydrological model. The hydrological simulation using APHRODITE as input obtained the most accurate runoff simulation among the six precipitation products.
4. APHRODITE shows the best performance among the six precipitation products. Thus, this product is a reliable choice for the hydrological and meteorological study in the MRB.

Declaration of Competing Interest

None.

Acknowledgments

The observed monthly meteorological data were provided by the China Meteorological Administration (<http://cdc.cma.gov.ac>). This research was supported by the Strategic Priority Research Program of Chinese Academy of Sciences, China (XDA20060402), the Natural Science Foundation of China (41922050) and the Youth Innovation Promotion Association, Chinese Academy of Sciences (No. 2018067).

References

- Akinsanola, A.A., Ogunjobi, K.O., Ajayi, V.O., et al., 2017. Comparison of five gridded precipitation products at climatological scales over West Africa. *Meteorol. Atmos. Phys.* 129 (6), 669–689.
- Alley, W.M., 1984. On the treatment of evapotranspiration, soil moisture accounting, and aquifer recharge in monthly water balance models. *Water Resour. Res.* 20 (8), 1137–1149.
- Ashouri, H., Hsu, K.L., Sorooshian, S., et al., 2015. PERSIANN-CDR: daily precipitation climate data record from multisatellite observations for hydrological and climate studies. *Bull. Am. Meteorol. Soc.* 96 (1), 69–83.
- Bai, P., Liu, X., 2018. Intercomparison and evaluation of three global high-resolution evapotranspiration products across China. *J. Hydrol.* 566, 743–755.
- Bai, P., Liu, X., Liu, C., 2018. Improving hydrological simulations by incorporating GRACE data for model calibration. *J. Hydrol.* 2018 (557), 291–304.
- Bai, P., Liu, X., Zhang, D., Liu, C., 2020. Estimation of the Budyko model parameter for small basins in China. *Hydrol. Process.* 34 (1), 125–138.
- Beck, H.E., Van Dijk, A.L.J.M., Levizzani, V., et al., 2017. MSWEP: 3-hourly 0.25 global gridded precipitation (1979–2015) by merging gauge, satellite, and reanalysis data. *Hydrol. Earth Syst. Sci.* 21 (1), 589–615.
- Beck, H.E., Wood, E.F., Pan, M., et al., 2019. MSWEP V2 global 3-hourly 0.1 precipitation: methodology and quantitative assessment. *Bull. Am. Meteorol. Soc.* 100 (3), 473–500.
- Behrang, A., Khakbaz, B., Jaw, T.C., et al., 2011. Hydrologic evaluation of satellite precipitation products over a mid-size basin. *J. Hydrol.* 397 (3–4), 225–237.
- Bitew, M.M., Gebremichael, M., 2011. Assessment of satellite rainfall products for streamflow simulation in medium watersheds of the Ethiopian highlands. *Hydrol. Earth Syst. Sci.* 15 (4), 1147.
- Boyle, D.P., Gupta, H.V., Sorooshian, S., 2000. Toward improved calibration of hydrologic models: combining the strengths of manual and automatic methods. *Water Resour. Res.* 36 (12), 3663–3674.
- Buarque, D.C., de Paiva, R.C.D., Clarke, et al., 2011. A comparison of Amazon rainfall characteristics derived from TRMM, CMORPH and the Brazilian national rain gauge network. *J. Geophys. Res.* 116 (D19).
- Bumke, K., König-Langlo, G., Kinzel, J., et al., 2016. HOAPS and ERA-Interim precipitation over sea: Validation against shipboard in-situ measurements. *Atmos. Measur. Techniq.* 9 (5), 2409–2423.
- Cai, X., Yang, Z.L., Fisher, J.B., et al., 2015. Integration of nitrogen dynamics into the Noah-MP land model v1. 1 for climate and environmental predictions. In: *Geoscientific Model Development Discussions*, 8(9).
- Chen, C.J., Senarath, S.U.S., Dima-West, I.M., et al., 2017. Evaluation and restructuring of gridded precipitation data over the Greater Mekong Subregion. *Int. J. Climatol.* 37 (1), 180–196.
- Chen, A., Chen, D., Azorin-Molina, C., 2018. Assessing reliability of precipitation data over the Mekong River Basin: a comparison of ground-based, satellite, and reanalysis datasets. *Int. J. Climatol.* 38 (11), 4314–4334.
- Ciach, G.J., Krajewski, W.F., Villarini, G., 2007. Product-error-driven uncertainty model for probabilistic quantitative precipitation estimation with NEXRAD data. *J. Hydrometeorol.* 8 (6), 1325–1347.
- Clark, M.P., Schaeffli, B., Schymanski, S.J., et al., 2016. Improving the theoretical underpinnings of process-based hydrologic models. *Water Resour. Res.* 52 (3), 2350–2365.
- Deb, K., Pratap, A., Agarwal, S., et al., 2002. A fast and elitist multiobjective genetic algorithm: NSGA-II. *IEEE Trans. Evol. Comput.* 6 (2), 182–197.
- Falck, A.S., Maggioni, V., Tomasella, J., et al., 2015. Propagation of satellite precipitation uncertainties through a distributed hydrologic model: a case study in the Tocantins-Araguaia basin in Brazil. *J. Hydrol.* 527, 943–957.
- Fernandez, W., Vogel, R.M., Sankarasubramanian, A., 2000. Regional calibration of a watershed model. *Hydrol. Sci. J.* 45 (5), 689–707.
- Frei, C., Christensen, J.H., Déqué, M., Jacob, D., Jones, R.G., Vidale, P.L., 2003. Daily precipitation statistics in regional climate models: evaluation and intercomparison for the European Alps. *J. Geophys. Res.* 108 (D3).
- Funk, C., Peterson, P., Landsfeld, M., et al., 2015. The climate hazards infrared precipitation with stations—a new environmental record for monitoring extremes. *Sci. Data* 2 (1), 1–21.
- Gupta, H.V., Sorooshian, S., Yapo, P.O., 1999. Status of automatic calibration for hydrologic models: comparison with multilevel expert calibration. *J. Hydrol. Eng.* 4 (2), 135–143.
- Gupta, H.V., Kling, H., Yilmaz, K.K., Martinez, G.F., 2009. Decomposition of the mean squared error and NSE performance criteria: implications for improving hydrological modelling. *J. Hydrol.* 377 (1), 80–91.
- Harris, I., Jones, P.D., Osborn, T.J., Lister, D.H., 2014. Updated high-resolution grids of monthly climatic observations—the CRU TS3.10 dataset. *Int. J. Climatol.* 34 (3), 623–642.
- Hirpa, F.A., Gebremichael, M., Hopson, T., 2010. Evaluation of high-resolution satellite precipitation products over very complex terrain in Ethiopia. *J. Appl. Meteorol. Climatol.* 49 (5), 1044–1051.
- Houghton, J., Townshend, J., Dawson, K., et al., 2012. The GCOS at 20 years: the origin, achievement and future development of the Global Climate Observing System. *Weather* 67 (9), 227–235.
- Hsu, K., Gao, X., Sorooshian, S., et al., 1997. Precipitation estimation from remotely sensed information using artificial neural networks. *J. Appl. Meteorol.* 36 (9), 1176–1190.
- Kidd, C., Becker, A., Huffman, G.J., et al., 2017. So, how much of the Earth's surface is covered by rain gauges? *Bull. Am. Meteorol. Soc.* 98 (1), 69–78.

- Kingston, D.G., Thompson, J.R., Kite, G., 2011. Uncertainty in climate change projections of discharge for the Mekong River Basin. *Hydrol. Earth Syst. Sci.* 15 (5), 1459–1471.
- Klemeš, V., 1986. Operational testing of hydrological simulation models. *Hydrol. Sci. J.* 31 (1), 13–24.
- Li, Z., Yang, D., Gao, B., et al., 2015. Multiscale hydrologic applications of the latest satellite precipitation products in the Yangtze River Basin using a distributed hydrologic model. *J. Hydrometeorol.* 16 (1), 407–426.
- Lutz, A., Terink, W., Droogers, P., et al., 2014. Development of Baseline Climate Data Set and Trend Analysis in the Mekong Basin. Mekong River Commission, Vientiane, Laos, pp. 1–127.
- Martinez, G.F., Gupta, H.V., 2010. Toward improved identification of hydrological models: a diagnostic evaluation of the “abcd” monthly water balance model for the conterminous United States. *Water Resour. Res.* 46 (8).
- Mei, Y., Anagnostou, E.N., Nikolopoulos, E.L., et al., 2014. Error analysis of satellite precipitation products in mountainous basins. *J. Hydrometeorol.* 15 (5), 1778–1793.
- Michaelides, S., Levizzani, V., Anagnostou, E., et al., 2009. Precipitation: measurement, remote sensing, climatology and modeling. *Atmos. Res.* 94 (4), 512–533.
- Moriyas, D.N., Arnold, J.G., Van Liew, M.W., Bingner, R.L., Harmel, R.D., Veith, T.L., 2007. Model evaluation guidelines for systematic quantification of accuracy in watershed simulations. *Trans. ASABE* 50 (3), 885–900.
- MRC, 2010. State of the Basin Report 2010. Mekong River Commission, 1728. Lao PDR, Vientiane, p. 3248.
- Nash, J.E., Sutcliffe, J.V., 1970. River flow forecasting through conceptual models part I—a discussion of principles. *J. Hydrol.* 10 (3), 282–290.
- New, M., Hulme, M., Jones, P., 2000. Representing twentieth-century space–time climate variability. Part II: Development of 1901–96 monthly grids of terrestrial surface climate. *J. Clim.* 13, 2217–2238.
- Pech, S., Sunada, K., 2008. Population growth and natural-resources pressures in the Mekong River Basin. *AMBIO* 37 (3), 219–224.
- Piesse, M., 2016. Livelihoods and food security on the Mekong River. In: Future Direction International, Strategic Analysis Paper (May 26, 2016). Accessed June, 13).
- Prigent, C., 2010. Precipitation retrieval from space: an overview. *Compt. Rendus Geosci.* 342 (4–5), 380–389.
- Rudolf, B., Becker, A., Schneider, U., et al., 2010. The new “GPCC Full Data Reanalysis Version 5” providing high-quality gridded monthly precipitation data for the global land-surface is public available since December 2010. In: GPCC Status Rep.
- Salathé Jr., E.P., 2003. Comparison of various precipitation downscaling methods for the simulation of streamflow in a rainshadow river basin. *Int. J. Climatol.* 23 (8), 887–901.
- Schamm, K., Ziese, M., Becker, A., et al., 2014. Global gridded precipitation over land: a description of the new GPCC First Guess Daily product. *Earth Syst. Sci. Data* 6 (1), 49.
- Schneider, Udo, Becker, Andreas, Finger, Peter, Meyer-Christoffer, Anja, Ziese, Markus, 2018. GPCC Full Data Monthly Product Version 2018 at 0.25°: Monthly Land-surface Precipitation From Rain-Gauges built on GTS-based and Historical Data.
- Shao, R., Zhang, B., Su, T., Long, B., Cheng, L., Xue, Y., Yang, W., 2019. Estimating the increase in regional evaporative water consumption as a result of vegetation restoration over the Loess Plateau, China. *J. Geophys. Res.* 124 (22), 11783–11802.
- Srinivas, N., Deb, K., 1994. Multiobjective optimization using nondominated sorting in genetic algorithms. *Evol. Comput.* 2 (3), 221–248.
- Tapiador, F.J., Turk, F.J., Petersen, W., et al., 2012. Global precipitation measurement: methods, datasets and applications. *Atmos. Res.* 104, 70–97.
- Thomas, H., 1981. Improved Methods for National Water Assessment. Report WR15249270. US Water Resource Council, Washington, DC.
- Tian, W., Liu, X., Liu, C., et al., 2018. Investigation and simulations of changes in the relationship of precipitation–runoff in drought years. *J. Hydrol.* 565, 95–105.
- Tolson, B.A., Shoemaker, C.A., 2007. Dynamically dimensioned search algorithm for computationally efficient watershed model calibration. *Water Resour. Res.* 43 (1), 208–214.
- Wan, Z., Zhang, K., Xue, X., et al., 2015. Water balance-based actual evapotranspiration reconstruction from ground and satellite observations over the conterminous United States. *Water Resour. Res.* 51 (8), 6485–6499.
- Werth, S., Güntner, A., Petrovic, S., Schmidt, R., 2009. Integration of GRACE mass variations into a global hydrological model. *Earth Planet. Sci. Lett.* 277 (1–2), 166–173.
- Xie, P., Arkin, P.A., 1996. Analyses of global monthly precipitation using gauge observations, satellite estimates, and numerical model predictions. *J. Clim.* 9, 840–858.
- Yang, T., Asanjan, A.A., Welles, E., et al., 2017. Developing reservoir monthly inflow forecasts using artificial intelligence and climate phenomenon information. *Water Resour. Res.* 53 (4), 2786–2812.
- Yatagai, A., Kamiguchi, K., Arakawa, O., et al., 2012. APHRODITE: constructing a long-term daily gridded precipitation dataset for Asia based on a dense network of rain gauges. *Bull. Am. Meteorol. Soc.* 93 (9), 1401–1415.
- Zhang, B., He, C., 2016. A modified water demand estimation method for drought identification over arid and semiarid regions. *Agric. For. Meteorol.* 230, 58–66.
- Zhang, D., Liu, X., Bai, P., 2019. Assessment of hydrological drought and its recovery time for eight tributaries of the Yangtze River (China) based on downscaled GRACE data. *J. Hydrol.* 568, 592–603.
- Zhang, B., Xia, Y., Huning, L.S., Wei, J., Wang, G., AghaKouchak, A., 2019a. A framework for global multicategory and multiscalar drought characterization accounting for snow processes. *Water Resour. Res.* 55 (11), 9258–9278.
- Zhang, B., AghaKouchak, A., Yang, Y., Wei, J., Wang, G., 2019b. A water-energy balance approach for multi-category drought assessment across globally diverse hydrological basins. *Agric. For. Meteorol.* 264, 247–265.
- Zhao, J., Wang, D., Yang, H., Sivapalan, M., 2016. Unifying catchment water balance models for different time scales through the maximum entropy production principle. *Water Resour. Res.* 52 (9), 7503–7512.